CO_2 fluid inclusions in ultramafic xenoliths from the Iblean Plateau, Sicily, Italy

B. De Vivo, A. Lima

Dipartimento di Geofisica e Vulcanologia, Largo S. Marcellino 10, 80138 Napoli, Italy

AND

V. Scribano

Istituto di Scienze della Terra, Corso Italia 55, 95129 Catania, Italy.

Abstract

The Iblean Plateau (Southeastern Sicily, Italy) consists of a thick Meso-Cenozoic carbonate sequence with interbedded volcanic horizons (alkaline and tholeiitic basalts). The alkaline basalts contain ultramafic (peridotites and pyroxenites) and mafic xenoliths. The peridotites are spinel-bearing lherzolites and lherzolitic harzburgites, with porphyroblastic to protogranular texture. Pyroxenites consist of Cr-diopside-bearing and Al-augite-bearing websterites. The mineral chemistry of the nodules indicates temperatures between 700 and 1050 °C.

Fluid inclusions containing CO_2 and (sometimes) various proportions of silicate glass have been studied in olivine, orthopyroxene and clinopyroxene. The secondary inclusions occur as trails of CO_2-rich inclusions, often cross-cutting deformation lamellae. The few primary inclusions, generally empty, show clear evidence of decrepitation. Of the 390 inclusions examined, 97% homogenized to the liquid phase (Th → L = −43.9 to +30.9 °C); 3% homogenized to the vapour phase (Th → V = +20.5 to +30.3 °C, yelding CO_2 densities in the range 0.20–1.13 g/cm^3. Assuming a trapping temperature of 1100 °C, the corresponding trapping pressure for a pure CO_2 system lies in the range 0.6–11.0 kbar, i.e. a depth of ~2.2 to 42 km.

The majority of CO_2 trapping events in the xenoliths occurred from 2.2 to 11.0 kbar, with no major trapping events at pressures less than 2.3 kbar, indicating the absence of a shallow magma reservoir below the Iblean Plateau.

Keywords: CO_2, fluid inclusions, ultramafic xenoliths, Iblean Plateau, Sicily.

Introduction

We have analysed fluid inclusions in four ultramafic xenoliths from alkaline lavas of the Iblean Plateau (Sicily), in order to examine the physical conditions of nodule genesis (De Vivo *et al.*, 1988, and references therein; Pasteris, 1987). Ultramafic xenoliths transported from the mantle into the upper crust represent a unique source of information about the fluid regime, the *PT* conditions, and the oxygen fugacity of the processes taking place in the upper mantle. In this study, data on fluid inclusions have been used to characterize the pressure and temperature (*P–T*) history of ultramafic xenoliths during their ascent to the surface.

Geological outlines

The Iblean Plateau (southeastern Sicily) forms the northern portion of the Pelagian Block, a sector of the African Plate margin, and consists of a Meso-Cenozoic carbonate sequence, with interbedded volcanic horizons (Fig. 1). The oldest outcropping terrains are Upper Cretaceous in age, whereas Upper Triassic carbonates and volcanic levels have been reached by the deepest drill holes in the area. There is no information on the lithology of the pre-Triassic basement.

The depth of the Moho is estimated to be about 30 km beneath the Iblean Plateau, decreasing to less than 20 km beneath the central portion of the

Mineralogical Magazine, June 1990, Vol. 54, pp. 183–94

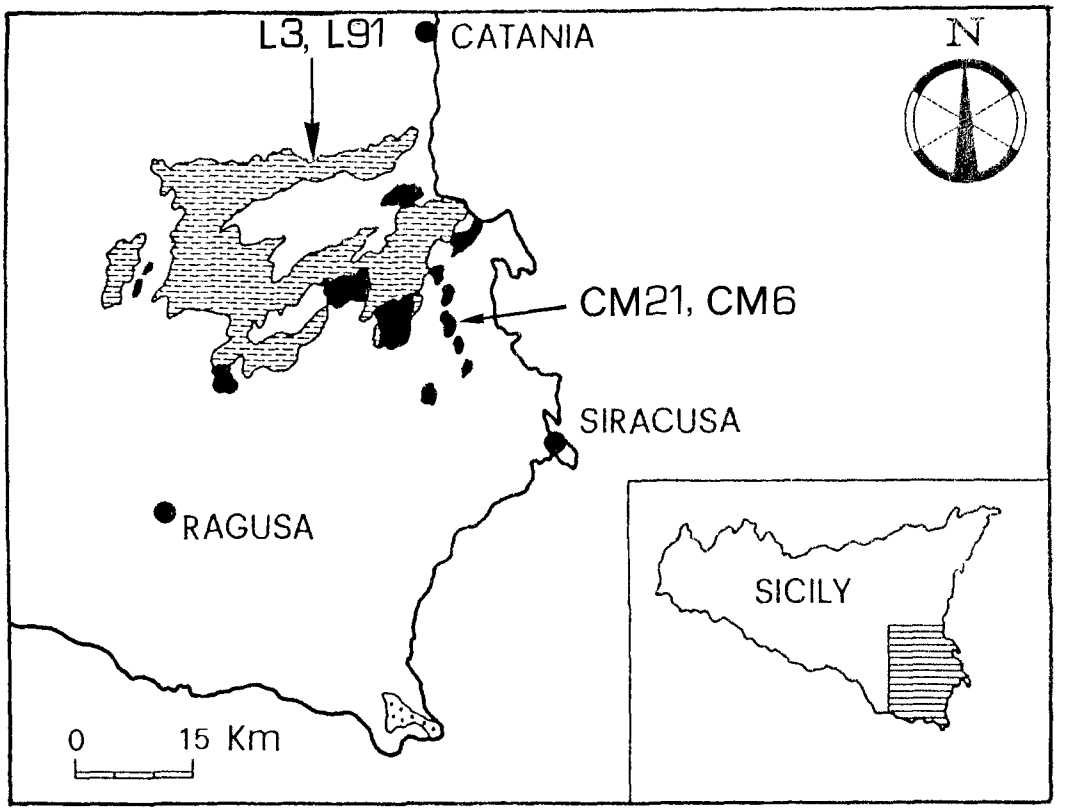

FIG. 1. Geological sketch of Iblean volcanic terrains (from Lentini *et al.*, 1987). Dotted area, Upper Cretaceous volcanic rocks; black, Upper Miocene tuff-breccia pipes and pyroclastic flow deposits; hatched areas, Plio-Pleistocene lava flows.

Pelagian Block (Central Mediterranean Sea), where active rift systems occur (Lentini *et al.*, 1987, and references therein).

Most of the Iblean volcanic rocks outcrop in the northeastern portion of the plateau, their ages ranging from Upper Miocene to Pleistocene. Miocene volcanic terrains consist of tuff-breccia pipes and related pyroclastic-flow deposits, with subordinate lava flows and dykes. The tuff-breccia consists of juvenile clasts (1 to 25 mm in size) of alkaline-mafic lava and a number of polygenetic xenoliths, which probably represent a 'cross section' through the lithosphere. The nodules, 1 to 20 cm in size and often exceeding 20 vol.% of the breccia, represent almost pristine deep-seated material; this is inferred from the lack of significant reactions with the host lava, presumably due to rapid, diatreme-type emplacement at relatively low eruption temperatures.

Plio-Pleistocene volcanic rocks consists of fissure-type lava flows of basaltic composition, with both alkaline and tholeiitic affinities. Deep-seated nodules were found only in lavas of the alkaline suite. An unusual nodule abundance occurs in the Quaternary lava from the northern margin of the Plateau.

The Iblean nodules may be divided into two main groups: (1) the ultramafic group, consisting mostly of mantle peridotites and pyroxenites, and (2) the feldspar-bearing group, which comprises lower crustal mafic granulites and rare felsic crystalline rocks (Scribano, 1986; 1987*a*).

Petrologic outlines of the Iblean ultramafic nodules

The peridotite nodules consist of spinel-bearing harzburgites and subordinate lherzolites, with texture varying from protogranular to porphyroclastic (following the classification of Mercier and Nicolas, 1975, and Harte, 1977). The protogranular texture occurs mostly in peridotites from the Miocene diatremes; the porphyroclastic texture,

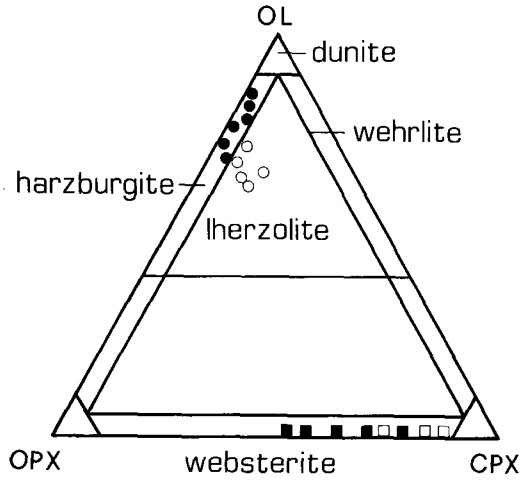

FIG. 2. Olivine (Ol)–orthopyroxene (Opx)–clinopyroxene (Cpx) modal proportions of Iblean ultramafic xenoliths. Full circle, peridotites from Plio-Pleistocene lavas; open circles, peridotites from Miocene tuff-breccia pipes; full squares, Cr–Di websterites; open squares, Al–Aug websterites.

however, is more common in nodules from the Pleistocene lavas.

The websterite nodules may be divided into two groups on the basis of their mineral chemistry: a Cr-diopside-bearing group and an Al-augite-bearing group (Fig. 2). All the Iblean websterites are spinel-bearing and often they contain Ni–Fe sulphides and pargasitic amphibole as accessory minerals. Most of the websterites display an inequigranular polygonal texture, due to orthopyroxene porphyroclasts 'coated' with ribbon-like augite neoblasts. Exsolution lamellae in pyroxenes are very common in all the Iblean websterites. Representative mineral and whole-rock analyses of Iblean peridotites and websterites are reported in Tables 1 and 2.

The textures and mineral chemistry of the Iblean ultramafic nodules are consistent with those of mantle xenoliths world-wide (Nixon, 1987, and references therein). Mineral and whole-nodule chemistry suggests that the Iblean peridotites have undergone significant depletion of their 'basaltic' constituents through time; as a rule, the harzburgites are more 'barren' than lherzolites. The peridotites equilibrated within the spinel–pyrolite field. The corresponding interval of equilibration pressure, as deduced from published experimental results on the CMAS system (Gasparik, 1984), ranges between 0.5 and 1.8 GPa (15–54 km depth); unfortunately, this interval is too wide for many interpretation purposes. The associated ranges of equilibration temperatures, determined from the partitioning of Cr–Al between coexisting spinel and orthopyroxene (Sachtleben and Seck, 1981) and of Mg–Fe partitioning between olivine and spinel (Fabries, 1979), varies from 700 to 1050 °C (Scribano, 1987*a*).

The websterite nodules of the Cr–Di group are interpreted as products of the fractional crystallization of 'primary' magmatic liquids, probably forming dykes and pods in the upper-mantle peridotites (Scribano, 1987*b*).

The Al-Aug websterites may represent more advanced stages of fractionation of the 'primary' magmatic liquid; this is suggested by the increase of relatively incompatible elements (Ti, Al) in the pyroxene and the modal increase of Al-spinel. Temperature estimates for the websterites yield a temperature interval of 850 and 1100 °C on the basis of several published geothermometers (Lindsley, 1983; Wood and Holloway, 1984; Gasparik, 1984, 1987). It is emphasized here that the two-pyroxene geothermometry is suitable only for pyroxene pairs of the Cr–Di group, owing to their relatively low contents of 'other' end-members. In addition, the *P–T* phase relations in the CMAS system imply, for the spinel-websterite mineral assemblage, an olivine-saturated surface (spinel-lherzolite field) or an anorthite-saturated surface (spinel-gabbro field). The first condition appears reasonable for the Iblean Cr–Di websterites, since the chemistry of their pyroxenes shows a close similarity with pyroxenes from peridotites (Table 1) (Scribano, 1987*c*).

Studied samples

Four nodules were selected for fluid inclusion studies. Samples L3 and L91 consist of harzburgites from a Quaternary ankaramite lava in the northern margin of the Iblean Plateau; samples CM6 and CM21 are websterites of the 'Cr-diopside-bearing group' from a Miocenic diatreme 2 km north of Melilli village (Fig. 1).

The texture of the harzburgite nodules is intermediate between the protogranular and the porphyroclastic; olivine porphyroclasts (2–4 mm in size) and subordinate enstatite grains are bounded by polygonal subgrains which make up about 25 vol.% of the nodule. However there is no evidence of foliation. Brownish chromian spinel occurs either as 'worms' interfingered with pyroxene grains or as holly-leaf grains located between the coarse silicate grains. Accessory Cr-diopside (5 vol.%) occurs in one of the studied samples (L91). Glassy 'blebs' are very common (Scribano, 1986). Microlaths of quench-diopside and carbo-

TABLE 1 - Representative mineral chemistry (ranges) of Iblean ultramafic nodules. LHZ.HZB: Lherzolite and harzburgite; Cr-Di WEB: Websterite of the Cr-diopside-bearing group; Al-Aug WEB: Websterite of the Al-Augite-bearing group. Microprobe analyses from Scribano 1986, 1987.

	LHZ-HZB	Cr-Di WEB	Al-Aug WEB
OLIVINE			
Fo (mol%)	90 - 91		
SPINEL			
Al2O3 (wt%)	16 - 36	50 - 56	36 - 65
Cr/(Cr+Al)	0.3 - 0.7	0.07 - 0.35	0 - 0.1
ORTHOPYROXENE			
Al2O3 (wt%)	0 - 3	4 - 5	4.0 - 6.4
CaO (wt%)	0 - 0.9	0.3 - 1.0	0.5 - 1.2
Cr2O3 (wt%)	0.25 - 0.45	0.3 - 0.6	0 - 0.19
Mg/(Mg+Fet)	0.90 - 0.92	0.90 - 0.92	0.80 - 0.87
CLINOPYROXENE			
Wo (mol%)	42 - 49	48 - 50	44 - 48
En (mol%)	50 - 51	48 - 50	44 - 53
Fs (mol%)	0 - 7	0 - 2	3 - 12
Al2O3 (wt%)	0 - 4	4 - 5	6 - 9
Cr2O3 (wt%)	0.8 - 1.5	0.7 - 1.0	0 - 0.4
TiO2 (wt%)	0 - 0.3	0.5 - 0.8	0.7 - 1.5

TABLE 2 - Representative whole-rock chemistry (ranges) of Iblean ultramafic nodules (wt.%).

	PERIDOTITE	Cr-Di WEB	Al-Aug WEB
SiO2	43 - 45	50 - 51	44 - 49
Al2O3	0.8 - 1.0	4 - 5	8 - 15
FeO	6 - 7	3 - 5	6 - 8
MgO	40 - 42	19 - 23	17 - 19
CaO	1.2 - 3.5	14 - 18	15 - 17
TiO2	0 - 0.4	0.3 - 0.6	0.9 - 1.2
Na2O	0 - 0.1	0.5 - 0.9	0.5 - 0.9

nates are often associated with the above-mentioned glassy blebs. Carbonates also occur as veinlets in the rock and they replace some of the olivine grains.

The two websterite nodules show inequigranular polygonal texture, consisting of coarse-equant grains of Cr-diopside (70 vol.%) with smaller orthopyroxene grains (25 vol.%). Exsolved lamellae of Ca-rich from Ca-poor pyroxene (and vice-versa) and spinel blades are ubiquitous in pyroxenes. Aluminous spinel and Ni–Fe sulphides complete the websterite modal assemblage. Additionally, in one of the studied samples (CM6), yellow chromian pargasite partially replaces one of the diopside grains.

Experimental methods

The samples were studied (at the Dipartimento di Geofisica e Vulcanologia, Napoli) using doubly polished sections of about 250 μm in thickness and a Chaix Meca heating/freezing stage (Poty *et al.*, 1976), modified as described by Cunningham and Corollo (1980).

The analytical techniques are the same as described by Roedder (1983) and Belkin *et al.* (1985). The calibration was made at −56.6, −6.0, 0, +10, and +51.1 °C. Near the vapour–liquid homogenization temperature, the precision of the stage was ±0.1 °C, with a rate of heating of about 0.1 °C per minute. The accuracy was difficult to assess in the range +28 to +31 °C. In the range −60 to −53 °C the precision is ±1.0 °C; the uncertainty of the CO_2 triple point (−56.6 °C) is about ±1.0 °C.

To check for the presence of additional components besides CO_2, Raman spectroscopy analyses (Microdil-28) (Burke and Lustenhouwer, 1987) on some selected inclusions have been performed at the Vrije Universiteit Amsterdam.

Occurrence of fluid inclusions

Although most of the fluid inclusions measured represent the trapping of only supercritical CO_2, a minority represent the trapping of two immiscible fluids, silicate melt and supercritical CO_2, sometimes with sulphide. At high pressure, the CO_2 fluid is miscible with silicate melt but, after sufficient decompression and, much more effectively, upon cooling, it can exsolve to form a separate phase. At room temperature, most of the inclusions consist of supercritical CO_2; biphase (L + V) inclusions are rare.

All our results refer to microthermometric measurements carried out on CO_2 inclusions, which have been used as a geobarometer. No temperature data have been obtained from the melt inclusions. The compositions were determined by various tests, using triple-point melting, critical phenomena and Raman analyses.

CO_2 inclusions are equally distributed among olivine, clinopyroxene and orthopyroxene. This distribution is different from that described by Francis *et al.* (1986) who report a significant decrease of CO_2 inclusions from clinopyroxene to orthopyroxene, olivine and spinel in a xenolith suite from the western margin of North America, in addition to a relative decrease in the amount of CO_2 inclusions from pyroxenite, websterite, spinel lherzolite, to harzburgite and dunite.

Most of the inclusions have a 'mature' aspect (Roedder, 1983), i.e. they have small and equant dimensions and are distributed mostly along intracrystalline or, subordinately, along intercrystalline fractures, which clearly denote their secondary origin (Fig. 3A). The microfracturing in the host crystals of the xenoliths is considered to have formed in response to decompression and thermal stresses during magma migration toward the surface which, according to Spera (1984), occurs by fracture as opposed to a diapiric mechanism (plastic flow). Silicate liquids saturated in CO_2 (depending on the ratio gas/glass) can migrate into these microfractures during transport to the surface; CO_2 alone, however, would tend to move in the opposite direction, from inclusions to the magma, due to overpressure and decrepitation effects (Andersen *et al.*, 1984). The fluids trapped in these microfractures and cracks are thus preserved as fluid inclusions. In addition to these immiscible fluids (melts + CO_2), occasional dark globules, interpreted as possible sulphides, have also been found (Fig. 3H, I, L). Such sulphides, occurring in melt + CO_2 inclusions (De Vivo *et al.*, 1988; Solovova *et al.*, 1985) in ultramafic xenoliths, are thought to be derived from an immiscible sulphide liquid formed during partial melting of mantle material (Dromgoole and Pasteris, 1985). A somewhat different interpretation of the formation of sulphide + CO_2 inclusions is given by Andersen *et al.* (1987). These authors suggest that fractional crystallization of basaltic magma in the uppermost mantle dumps S, Ni, Cu, Co, etc. as part of the general process of mantle metasomatism.

Compared with similar studies of ultramafic xenoliths (e.g. De Vivo *et al.*, 1988; Belkin and De Vivo, 1989) dendritic 'immature' inclusions are not very frequent (density from 0.20 to 0.46 g/cm^3) (Fig. 3B). This type of inclusion is generally associated with the trapping of CO_2 and silicate melt; apparently, therefore, such fluids can only have had a minor presence in the Iblean xenoliths.

Haloes of tiny secondary inclusions occur commonly around large, primary, empty inclusions (Fig. 3G, L). They develop into planes of spherical inclusions, sometimes forming a tubular or vermicular network, and were formed through a recrystallization process, after decrepitation and emptying of the primary inclusions. Decrepitation is the result of internal overpressure during ascent to the surface, and occurs when the internal pressure in the inclusions exceeds, by an amount equal to the tensile strength of the crystal, the lithostatic pressure acting on the host mineral (Roedder, 1981).

The size of the measured inclusions ranges from 2 to 40 μm, with the very great majority between 2 and 4 μm. Inclusions of less than 2 μm in size are extremely abundant, but for obvious optical problems were not measurable.

Microthermometric results

The triple points (i.e. T_m–CO_2) of 201 frozen inclusions were found to be in the range −55.6 to −57.6 °C (Fig. 4), with 86% of the measurements at −56.6 °C, indicating a pure CO_2 system. Raman analyses confirm that the system is made up of CO_2, with no other components (e.g. CO, N_2, H_2O, CH_4) present, at least above the instrumental detection limit (0.04 mole % for CH_4; 0.2 mole % for N_2) (Burke and Lustenhouwer, 1987).

Fig. 5 shows the CO_2 density distribution for the CO_2 fluid inclusions, determined from homogenization temperature and behaviour (Th → L; Th → V). Of the 390 analysed inclusions 97% homogenized to the liquid phase at temperatures ranging from −43.9 to +30.9 °C. Only 11 inclusions homogenized to the vapour phase at temperatures from +20.5 to +30.3 °C. These are mostly the 'immature' inclusions, often associated with glass. The density histogram shows a bimodal dis-

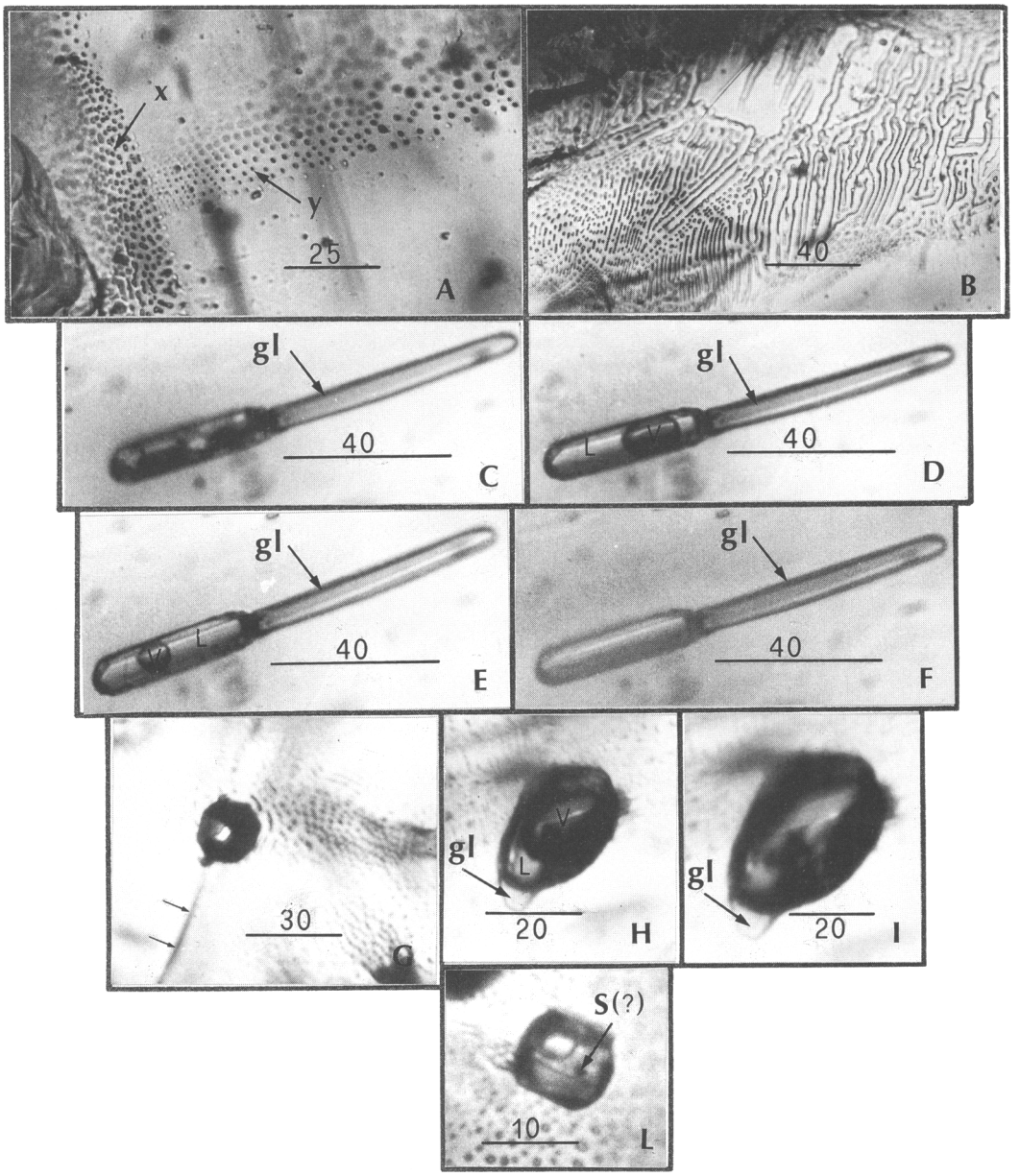
x
y
25
A
40
B
gl
40
C
gl
L
V
40
D
gl
V
L
40
E
gl
40
F
30
G
gl
V
L
20
H
gl
20
I
S(?)
10
L

tribution, with two distinct peaks at 0.77 and 1.02 g/cm^3. Such a distribution is common in this type of data (Bilal and Touret, 1976; Andersen *et al.*, 1984; De Vivo *et al.*, 1988). Only a very few values, from inclusions homogenizing in the vapour phase, are distributed in the low-density area, with values between 0.20 and 0.36 g/cm^3.

Fig. 5 shows that the high density inclusions occur, without any preferential distribution, in all the three mineral phases analysed (olivine, clinopyroxene and orthopyroxene), although clinopyroxene and orthopyroxene contain more high-density inclusions than olivine (no Th → L occurs in olivine below −24 °C, whereas more than 50 such inclusions occur in clinopyroxene and orthopyroxene between −24 °C and −43 °C). This result contrasts with some other studies of ultramafic xenoliths (De Vivo *et al.*, 1988), which indicated olivine to be the preferential host mineral for the high-density inclusions, suggesting that, compared with clinopyroxene and orthopyroxene, olivine has a relatively higher mechanical strength and so is better able to withstand changes in pressure during ascent. Other studies, consistent with our results, indicate that the greatest densities of inclusions are found in pyroxenes (Andersen *et al.*, 1984). The high-density CO_2 inclusions are clearly correlated with the size of the inclusions. The very small ones (*c.* 2 μm) in fact always indicate the highest density values, showing that they are more resistant to decrepitation than larger ones (Roedder, 1984).

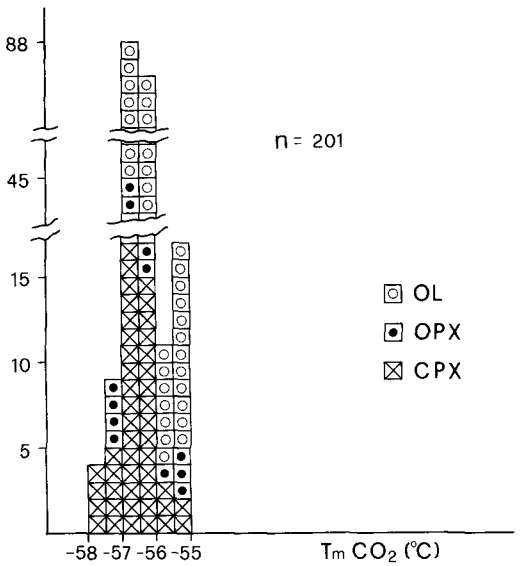

FIG. 4. Melting temperature (T_m °C–CO_2) of 201 CO_2 fluid inclusions.

Discussion and conclusions

P and T of trapping. The Raman analyses and triple point measurements of frozen inclusions both suggest that the trapping pressures estimated from the isochores for the fluids in our samples closely approximate the isochores for pure CO_2. On the other hand, reactions between the fluid and the cavity walls, which produce a change of both the density and the composition of the fluids remaining in the inclusions, are in one case indicated by the presence of magnesite daughter minerals (Burke, pers. comm.), probably resulting from reactions between H_2O, CO_2 and possibly CO. Carbonates have been found, as well, associated with glass and as veinlets replacing olivine grains. It is possible, therefore, that the pure CO_2 fluids may have evolved, at least in part, through decrepitation and reaction mechanisms, from more complex CO_2–H_2O or CO_2–H_2O–CO primary fluids (Andersen *et al.*, 1984). The fact that H_2O might have been removed by reactions

FIG. 3. (A) Cross-cutting trails of CO_2 fluid inclusions in clinopyroxene, with 'mature' aspect; sample CM6: the inclusions of the fracture *x* have density values much lower (0.84/0.86 g/cm^3, i.e. 5.2/5.5 kbar) than the inclusions of the fracture *y* (0.94/1.04 g/cm^3, i.e. 6.8/9.0 kbar), indicating two different fracturing and healing events of the crystal during its ascent toward the surface. (B) Dendritic, 'immature' trail of CO_2 inclusions in clinopyroxene; sample CM6. (C, D, E, F) Secondary CO_2 inclusion wetting silicate melt, now glass (gl) in orthopyroxene; sample CM6; C—CO_2 solid at −100 °C; D—CO_2 (L) and CO_2 (V), at −10 °C; E—CO_2 (L) and CO_2 (V), at 12.5 °C; F—the same inclusion at 25 °C, after homogenization, which occurs in the liquid phase at 21.3 °C. (G) Typical primary empty CO_2 inclusion in clinopyroxene; sample CM6: the fracture crossing the inclusion (arrows) and the circular halo of tiny fluid inclusions show clearly that the inclusion has suffered decrepitation. (H, I) Secondary fluid inclusion in orthopyroxene, sample CM6, showing the presence of two immiscible coexisting phase: CO_2 and glass (gl); H—inclusion at 15 °C, with a defined meniscus separating liquid (L) and vapour (V) CO_2; I—the same inclusion at 32°C after homogenization in the liquid phase at 29.8 °C. (L) Primary CO_2 inclusion in clinopyroxene, sample 2HCM, which suffered partial decrepitation, as shown by the fracture crossing the inclusion and the circular halo of tiny inclusions. The inclusion homogenizes in the liquid phase at 25.5 °C. The dark globule (S?) might be a sulphide. Microphotographs in plane-polarized transmitted light; scale bars in micrometres.

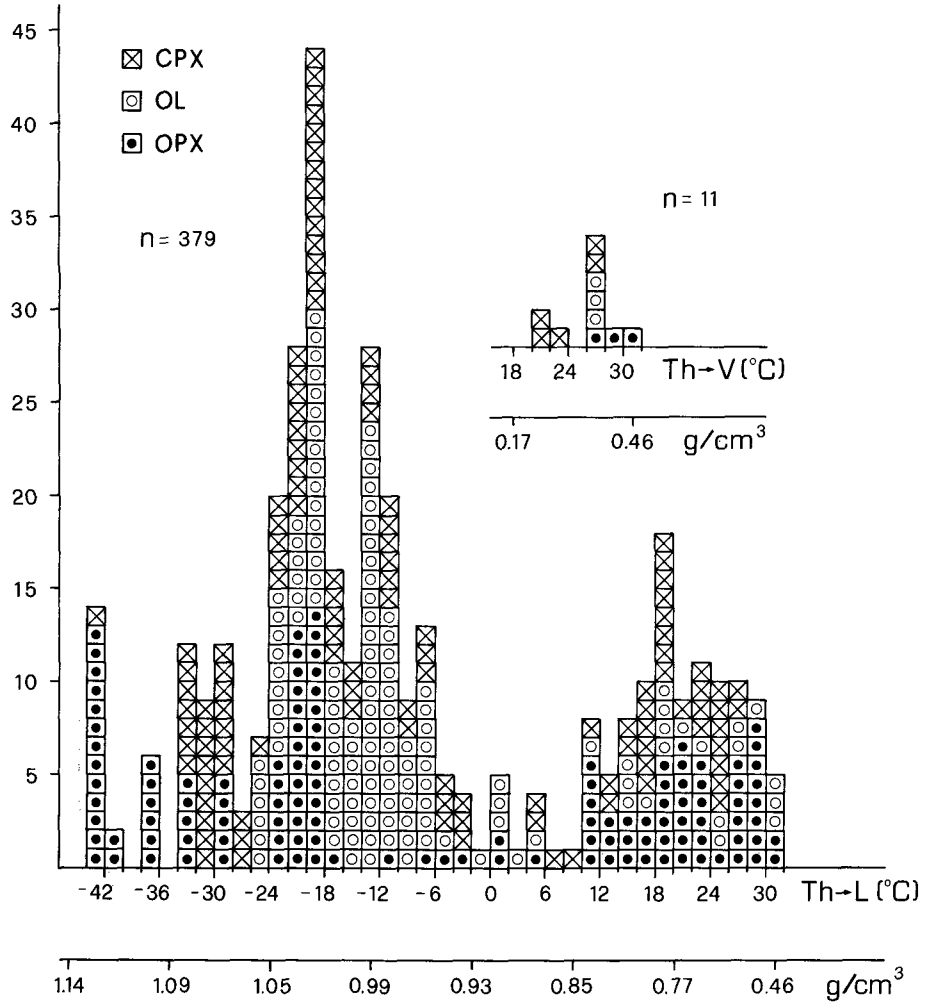

FIG. 5. Homogenization temperatures (Th °C) and density (g/cm^3) distribution of 390 CO_2 fluid inclusions. Density values are obtained assuming a pure CO_2 system.

is also confirmed by the presence of H_2O-bearing phases (amphibole) in the websterite nodules.

The trapping pressures estimated assuming a trapping temperature of 1100 °C, based on the mineral chemistry of the lherzolite nodules (Scribano, 1987) and a *T–V* (i.e. density) plot for a pure CO_2 system [using both experimental (Kennedy, 1954; Shmonov and Shmulovich, 1974) and calculated data (Kerrick and Jacobs, 1981)], are therefore minimum values, since both decrepitation and reaction between fluids in the inclusions and cavity walls increase the molar volume of the trapped fluids. On the other hand, the effect of impurities other than H_2O (i.e. CO or N_2), which reduce the isochore pressure for equal densities, is comparatively small (van den Kerkhof, 1988).

All the inclusions appear to have been trapped in the range 0.6–11.0 kbar with two major clusters between 2.3–6.5 kbar and 6.5–11.0 kbar (Fig. 6). It remains uncertain whether the prevailing pressure regime at the time of trapping was 'hydrostatic' (from a liquid lava column) or lithostatic (nodules crystallizing in sealed pockets, surrounded by country rocks). For this reason, the relationships between density of CO_2 inclusions and depth, are shown in Fig. 6 for both 'hydrostatic' (d = 2.7 g/cm^3) and lithostatic (d = 3.3 g/cm^3) pressure regimes.

The majority of CO_2 trapping events in the

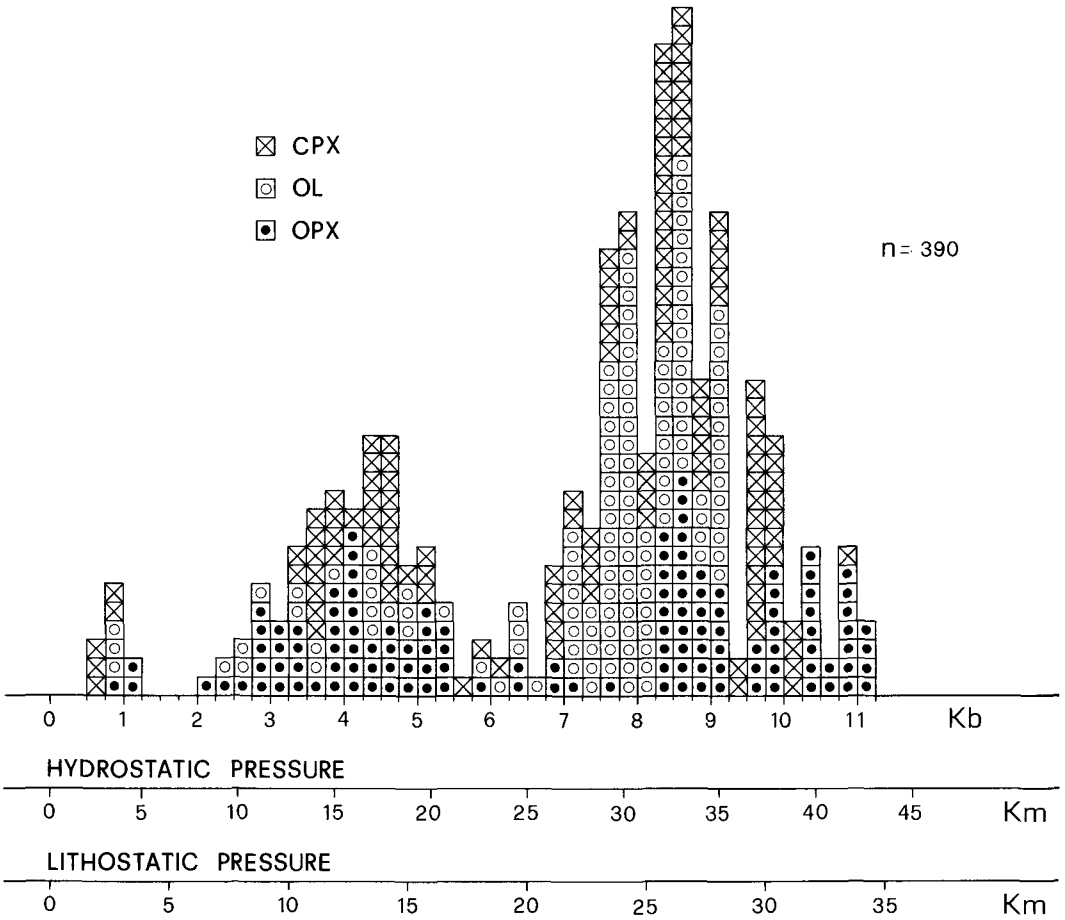

FIG. 6. Pressure (kbar) distribution, derived from CO_2 density values, assuming a trapping temperature of 1100 °C. Isobars from the modified Redlich–Kwong equation of Kerrick and Jacobs (1981). Depths in km assuming both hydrostatic ($d = 2.7\ g/cm^3$) and lithostatic ($d = 3.3\ g/cm^3$) pressure regimes.

xenoliths occurred between pressures from 2.3 to 11.0 kbar (~9–42 km) (Fig. 6). The two preferred populations, in the ranges 2.3–6.5 kbar and 6.5–11.0 kbar, might indicate the presence of large reservoirs of free fluid CO_2 located in the deep crust (~9–24 km depth) and in the upper mantle (~25–42 km depth), from which ascending magmas collected additional volatiles. The presence of other, very subordinate, inclusion trails suggests minor fracturing and healing events at very shallow depths. These late, 'surficial' inclusions, which generally trap CO_2 along with silicate melt, may have formed after xenolith degassing, the reduction of internal pressure in the inclusions allowing the infiltration of basaltic melt and volatiles from the host magma (Andersen *et al.*, 1984).

All the high-density inclusions have a very 'mature' aspect, indicating that a relatively long time was required for them to develop their shape (De Vivo *et al.*, 1988). This is especially true for the inclusions trapped below about 6.5 kbar (~25 km depth). The high frequency of interaction events between the magma and the xenoliths at depths between 9 and 42 km, in addition to the observation that a 'long' period was required for the inclusions to assume their present shape, might imply a very slow initial upward transport of the xenoliths in the magma, at least below 25 km depth, prior to explosive eruption.

Ascent rate of xenoliths. A slow initial upward ascent of the nodule-bearing magmas would also be consistent with the findings of similar fluid inclusion studies of ultramafic xenoliths at Oahu island, Hawaii (De Vivo *et al.*, 1988) and in Sardi-

nia, Italy (Belkin and De Vivo, work in progress). In the ultramafic xenoliths of Victoria, Australia, slow initial magma ascent is further suggested by a series of reactions to successively finer-grained, lower-pressure mineral assemblages (Griffin *et al.*, 1984). More specifically, Griffin *et al.* (1984) estimate that nodule-bearing magmas have ascent rates of ~0.1 m/s below ~10 kbar and of ~10 m/s above ~10 kbar. Such changes in velocity may be interpreted in terms of the ascent through small conduits (a few metres in diameter) of a magma containing a high concentration of nodules. Initially, magma ascent is driven essentially by buoyancy. Even though the rate of ascent is slow, the magma can still transport the nodules if it has a suitable non-Newtonian rheology (Sparks *et al.*, 1977). As shown by the presence of fluid inclusions, the deep magma must also be volatile-rich, possibly after having absorbed volatiles in the zone where the xenoliths originate (Griffin *et al.*, 1984). As a result, degassing begins at deep levels, accelerating the magma to a critical depth (probably represented by the brittle fractures which also characterize our lherzolite xenoliths) where the boiling of these fluids leads to crack propagation and, finally, to explosive velocities. In our nodules (Fig. 6) we observe relatively few high-density inclusions, both in clinopyroxene and orthopyroxene (9.5–11 kbar). A large increase in inclusion density occurs between 7.5 and 9 kbar, probably coinciding with a level of major gas release from the magma, which promotes the fracturing and a significant change in the ascent rate (the CO_2 inclusions found in this pressure range are tiny, ovoid and 'mature'). This finding is consistent with the conclusions of Griffin *et al.* (1984). A second gas release event occurs at about 4–5 kbar, associated with the zone of melt trapping; this corresponds to the last magma chamber for the rising basalt. The rate of ascent appears to have again changed significantly at about 2.5 kbar (~10 km), where explosive velocities were achieved, leading to eruption. At pressures less than about 2.5 kbar, the inclusions are always vermiform and 'immature'.

Two further implications of the preferred trapping depths concern the shallow magnatic feeding system and the origin of the CO_2 fluids. First, the lack of relevant CO_2 trapping events in the xenoliths at depths less than ~10 km suggests that no shallow magma reservoir has existed beneath the Iblean Plateau. Second, the high preferred trapping pressure of 11 kbar corresponds to a depth of about 42 km which, since it is greater than the depth of the Moho beneath Sicily (~30 km), suggests that the inclusions contain mantle CO_2.

Indeed, the presence of primary mantle CO_2 in our xenoliths would also be compatible with the relatively common occurrence of partial or complete decrepitation (the effect of partial decrepitation is to increase the volume available to the fluid and consequently to reduce the density) and subsequent sealing (Fig. 3L). Our data therefore strongly indicate that most of the CO_2 fluids were trapped at upper-mantle depths, so providing evidence of a free fluid phase at high P and T.

Mantle metasomatism. CO_2 fluid inclusions are the only direct samples of the free fluid phase in the mantle. They are extremely important because fluids dominated by CO_2, together with H_2O and small amounts of Cl, F and S species, are considered to provide an efficient mechanism for the metasomatic enrichment of the upper mantle in LIL elements (Andersen *et al.*, 1984; O'Reilly and Griffin, 1985). Such metasomatism is well recognized in upper-mantle peridotite xenoliths in kimberlites and basalts (Dawson, 1984). Although we do not yet have petrographic evidence of the development of a hydrous phase rich in incompatible elements to support the implications for mantle metasomatism (but see Belkin and De Vivo, 1989), our Iblean data do confirm that the free fluid degassing from the upper mantle is dominantly CO_2. This fluid is probably the residual phase of a larger volume of fluid, originally richer in H_2O and derived from a primitive reservoir of free fluid in the mantle (Andersen *et al.*, 1984). The CO_2 fluids may be liberated from the mantle reservoir, during episodes of magmatism or during crustal thinning and rifting, to induce granulite-facies metamorphism in the lower crust.

Acknowledgements

The authors are indebted to E. A. J. Burke (Vrije Universiteit of Amsterdam) for Raman analyses; to M. Cortini (Univ. of Napoli) and to C. Kilburn (Osservatorio Vesuviano, Napoli) for their useful comments on the manuscript; to G. Di Bitonto for drafting the illustrations. Constructive reviews by T. Andersen (Univ. of Oslo) and J. Touret (Vrije Universiteit of Amsterdam) helped improve the manuscript.

References

Andersen, T., O'Reilly, S. Y. and Griffihn, W. L. (1984) The trapped fluid phases in upper mantle xenoliths from Victoria, Australia: implications for mantle metasomatism. *Contrib. Mineral. Petrol.* **88**, 72–85.

—— Griffin, W. L. and O'Reilly, S. Y. (1987) Primary sulphide melt inclusions in mantle-derived megacrysts and pyroxenites. *Lithos* **20**, 279–94.

Belkin, H. E. and De Vivo, B. (1989) Glass, phlogopite,

and apatite in spinel peridotite xenoliths from Sardinia (Italy): evidence for mantle metasomatism. IACVEI Meeting, Santa Fe, NM, June 26–July 1, *Program with Abstracts*, p. 20.

———Roedder, E. and Cortini, M. (1985) Fluid inclusion geobarometry from ejected Mt Somma-Vesuvius nodules. *Am. Mineral.* **70**, 288–303.

Bilal, A. and Touret, J. (1976) Fluid inclusions in catazonal xenoliths from Bournac (Massif Central, France). *Bull. Mineral.* **99**, 134–9.

Burke, E. A. J. and Lustenhouwer, W. J. (1987) The application of a multichannel laser Raman microprobe (Microdil-28) to the analysis of fluid inclusions. *Chem. Geol.* **61**, 11–17.

Cunningham, C. G. and Corollo, C. (1980) Modification of a fluid inclusion heating freezing stage. *Econ. Geol.* **75**, 335–7.

Dawson, J. B. (1984) Contrasting types of upper mantle metasomatism? In: Kimberlites, v. II: The mantle and crust-mantle relationships, Proc. of the 'Third Int'l Kimberlite Conference' (J. Kornprobst, ed.) Elsevier, Amsterdam, pp. 289–294.

De Vivo, B., Frezzotti, M. L., Lima, A. and Trigila, R. (1988) Spinel lherzolite nodules from Oahu island (Hawaii): a fluid inclusion study. *Bull. Mineral.* **111**, 307–19.

Dromgoole, E. L. and Pasteris, J. D. (1985) Interpretation of the sulfide assemblages in a suite of xenoliths from Kilbourne Hole, New Mexico. *Geol. Soc. Am., Abstract with Programs.* **17**, 157.

Fabries, J. (1979) Spinel–olivine geothermometry in peridotite from ultramafic complexes. *Contrib. Mineral. Petrol.* **69**, 329–36.

Francis, D., Javoy, M., Nadeau, S. and Pineau, F. (1986) Upper mantle xenoliths along the north western margin of North America: Fluid inclusions and C and H isotopes. *Terra Cognita* **6**, 191–2.

Gasparik, T. (1984) Two-pyroxene thermobarometry with new experimental data in the system CaO–MgO–Al_2O_3–SiO_2. *Contrib. Mineral. Petrol.* **87**, 73–87.

——(1987) Orthopyroxene thermobarometry in simple and complex systems. Ibid. **96**, 357–70.

Griffin, W. L., Wass, S. Y. and Hollis, J. D. (1984) Ultramafic xenoliths from Bullenmerri and Gnotuk Maars, Victoria, Australia: Petrology of a subcontinental crust-mantle transition. *J. Petrol.* **25**, 53–87.

Harte, B. (1977) Rock nomenclature with particular relation to deformation and recrystallization textures in olivine-bearing xenoliths. *J. Geol.* **85**, 279–88.

Kennedy, G. C. (1954) Pressure–volume relations in CO_2 at elevated temperatures and pressures. *Am. J. Sci.* **252**, 225–41.

Kerrick, D. M. and Jacobs, G. K. (1981) A modified Redlich-Kwong equation for H_2O, CO_2 and H_2O–CO_2 mixtures at elevated pressures and temperatures. Ibid. **281**, 735–67.

Lentini, F., Grasso, M. and Carbone, S. (1987) *Introduzione alla geologia della Sicilia e guida all'escursione.* Università degli Studi di Catania, Istituto di Scienze della Terra. Catania, 60 pp.

Lindsley, D. H. (1983) Pyroxene thermometry. *Am. Mineral.* **68**, 477–93.

Mercier, J. C. and Nicolas, A. (1975) Textures and fabrics of upper-mantle peridotites as illustrated by xenoliths from basalts. *J. Petrol.* **16**, 454–87.

Nixon, P. H. (1987) *Mantle xenoliths.* Wiley J. & Sons, London, 563 pp.

O'Reilly, S. Y. and Griffin, W. L. (1985) The nature and role of fluids in the upper mantle: evidence in xenoliths from Victoria, Australia. Abstracts of Conf. on Stable Isotopes and Fluid Processes in Mineralization, Queensland, 10–12 July, p. 58–59.

Pasteris, J. D. (1987) Fluid inclusions in mantle xenoliths. In *Mantle Xenoliths* (Nixon, P. H., ed.) John Wiley & Sons, London, 691–707.

Poty, B., Leroy, J. and Jachimowicz, L. (1976) Un nouvel appareil pour la mesure des temperatures sous le microscope: l'installation de microthermometrie de Chaix Meca. *Bull. Mineral.* **99**, 182–6.

Roedder, E. (1981) Origin of fluid inclusions and changes that occur after trapping. In *Fluid inclusions: application to petrology* (Hollister, L. S. and Crawford, M. L., eds.) Mineral. Assoc. Canada Short Course, Calgary. **6**, 101–37.

——(1983) Geobarometry of ultramafic xenoliths from Loihi seamount, Hawaii, on the basis of CO inclusions in olivine. *Earth Planet. Sci. Lett.* **66**, 369–79.

——(1984) *Fluid inclusions.* Review in Mineralogy, Min. Soc. Am., **12**, 70–1.

Sachtleben, T. and Seck, H. A. (1981) Chemical control of Al-solubility in orthopyroxene and its implications on pyroxene geothermometry. *Contrib. Mineral. Petrol.* **78**, 157–65.

Scribano, V. (1986) The harzburgite xenoliths in a Quaternary basanitoid near Scordia (Hyblean Plateau, Sicily). *Rend. Soc. Ital. Mineral. Petrol.* **41**, 245–55.

——(1987*a*) The ultramafic and mafic nodule suite in a tuff-breccia pipe from Cozzo Molino (Hyblean Plateau, SE Sicily). Ibid. **42**, 203–17.

——(1987*b*) Deep-seated xenoliths in alkaline volcanic rocks from the Hyblean Plateau (SE Sicily). *Mem. Soc. Geol. Ital.* **38**, in press.

——(1987*c*) Origin of websterite nodules from some alkaline volcanic rocks of Hyblean Plateau (South Eastern Sicily). *Period. Mineral.* **56**, in press.

Shmonov, V. M. and Shmulovich, K. I. (1974) Molal volumes and equation of state of CO_2 at temperatures from 100 to 1000 °C and pressures from 2000 to 10 000 bars. *Dokl. Akad. Nauk SSSR* **217**, 935–8.

Solovova, I. P., Kovalenko, V. I., Naumov, V. B., Ryabchikov, I. D., Ionov, D. A. and Tsepin, A. I. (1985) Carbon dioxide–sulfide–silicate inclusions in clinopyroxenes from mantle xenoliths. Ibid. **285**, 199–202.

Sparks, R. S. J., Pinkerton, H. and Macdonald, R. (1977) The transport of xenoliths in magmas. *Earth Planet. Sci. Lett.* **35**, 234–8.

Spera, F. J. (1984) Carbon dioxide in petrogenesis III: role of volatiles in the ascent of alkaline magma with special reference to xenolith-bearing mafic lavas. *Contrib. Mineral. Petrol.* **88**, 217–32.

Van Den Kerkhof, A. M. (1988) *The system*

CO_2–CH_4–N_2 in fluid inclusions: theoretical modelling and geological applications. PhD thesis, Vrije Universiteit Amsterdam, 206 pp.

Wood, B. J. and Holloway, J. R. (1984) Thermodynamic model for subsolidus equilibria in the system CaO–Al_2O_3–SiO_2. *Geochim. Cosmochim. Acta*, **48**, 159–76.

[*Manuscript received 13 June 1989; revised 15 January 1990*]